

# LATTICE CONSTANTS OF SYNTHETIC CHALCANTHITE BY THE X-RAY PRECESSION TECHNIQUE USING A SINGLE MOUNTING OF THE CRYSTAL

D. JEROME FISHER, *University of Chicago, Chicago, Illinois.*

## ABSTRACT

Chalcanthite is herewith returned to its pre-Barker setting with  $\alpha$  and  $\beta$  obtuse,  $\gamma$  acute (rather than  $\beta$  and  $\gamma$  obtuse,  $\alpha$  acute), but otherwise no change except for refinements in detail. The  $x$ -ray precession technique as applied to a triclinic crystal with but a single mounting is described for (1) precession along two axes, and (2) precession along but a single axis. A new angle table has been prepared.

## INTRODUCTION

Following Romé de l'Isle's *Essai de Cristallographie* of 1772, chalcanthite ( $\text{CuSO}_4 \cdot 5\text{H}_2\text{O}$ ) has frequently<sup>1</sup> been used as a textbook example of a triclinic crystal, since it is readily available, at least in the synthetic condition, shows good prismatic habit, and has pronounced obliquity of crystal axes. For this reason, and because the relatively new  $x$ -ray precession technique (Buerger, 1944) seems ideally suited to the mineralogists' use for getting crystal angles, this paper has been prepared. The present study was made on a single crystal 0.4 by 0.6 by 1.5 mm. which was grown on the overnight cooling of a slightly supersaturated solution made from the C. P. salt. This work was started to supply material for use in a beginning course in  $x$ -ray crystallography; it seemed of sufficient interest to warrant some further study which yielded the results herein reported.

## ORIENTATION

While many orientations have been used for chalcanthite (Goldschmidt, 1918, vol. 5, p. 105), since 1908 when Groth (1908, vol. 2, pp. 419-421) appeared, Barker's setting has become quite standard.<sup>2</sup> However, Barth and Tunell (1933) noted the unconventionality of Barker's orientation, though they retained it. Later Donnay (1943 *a*) suggested certain more or less arbitrary rules for orienting crystals; it is desirable to adopt these in order to achieve some degree of uniformity. The rules seem good for reasons stated by Donnay, but also because they preserve

<sup>1</sup> For example, see Barker (1922, pp. 36-38; 1930), Goldschmidt (1934, pp. 63-65), Terpstra (1946, pp. 91, 101, 147-151, 156-166, 236, 297), Tutton (1911, pp. 286-302; 1922, pp. 282-298).

<sup>2</sup> Apparently Barker's setting was first published in 1905 by Groth (1905, p. 349).

the standard orientation of the soda plagioclase feldspars.<sup>3</sup> In accordance with these rules, chalcantinite is here reoriented from the Barker setting by reversing the signs on the ends of the  $[a]$  and  $[c]$  axes.<sup>4</sup> The transformation formula from Barker is simply  $\bar{1}00/010/00\bar{1}$ .

A typical habit of chalcantinite is shown in Fig. 4<sup>5</sup> in the two settings. The prismatic zone carries the plus and minus unit hemi-prisms as well as front and side pinacoids; this is terminated by the large unit tetartodipyramidal form which is  $\omega\{111\}$  in the Barker setting and  $p\{\bar{1}\bar{1}\bar{1}\}$

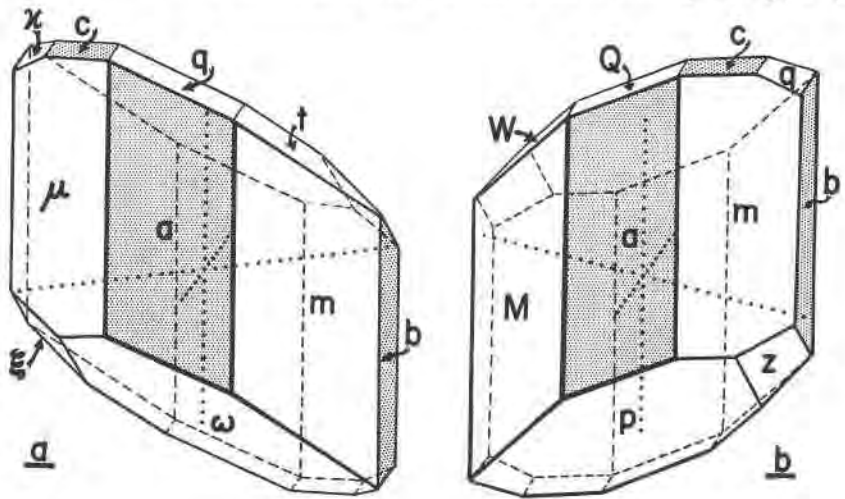


FIG. 4. Axonometric projections of chalcantinite in the (a) Barker setting, and (b) the old setting used in this paper. The pinacoids are stippled.

in the setting of this paper; the other terminal faces are generally quite small, but in the synthetic sample used in the present study  $z\{\bar{1}2\bar{1}\}$  was several times as large as  $p$ . Figure 5 is a gnomonogram showing the main terminal forms in the two settings. One setting goes to the other by inversion followed by rotation of  $180^\circ$  on the  $[b^*]$  axis.<sup>6</sup> This is simpler

<sup>3</sup> The suggestion of Donnay (1943b) that the lime plagioclases be reoriented is unfortunate, and goes against first principles governing the treatment of a high-temperature solid solution series. Orientation of triclinic crystals has recently been discussed by Milne and Nuffield (1951, pp. 401-407).

The orientation of chalcantinite used in this paper is adopted by Palache *et al.* (1951, p. 488).

<sup>4</sup> This results in the first orientation of Donnay (1943b, p. 511); the second one is erroneous, due to a misprint in Wyckoff.

<sup>5</sup> The numbers here assigned to tables, figures, and formulas are in continuation of the numbers used for the same purposes in the preceding paper (Fisher, 1952).

<sup>6</sup> Elements of the reciprocal lattice are designated by an asterisk. The reciprocal axes are normal to the three pinacoidal planes of the direct lattice. The axes of the direct lattice (the "crystal axes") are normal to the three "pinacoidal" planes of the reciprocal lattice;

than considering that one setting goes to the other by reflection in (010), since the crystal is assumed to have a center of symmetry. Thus one can

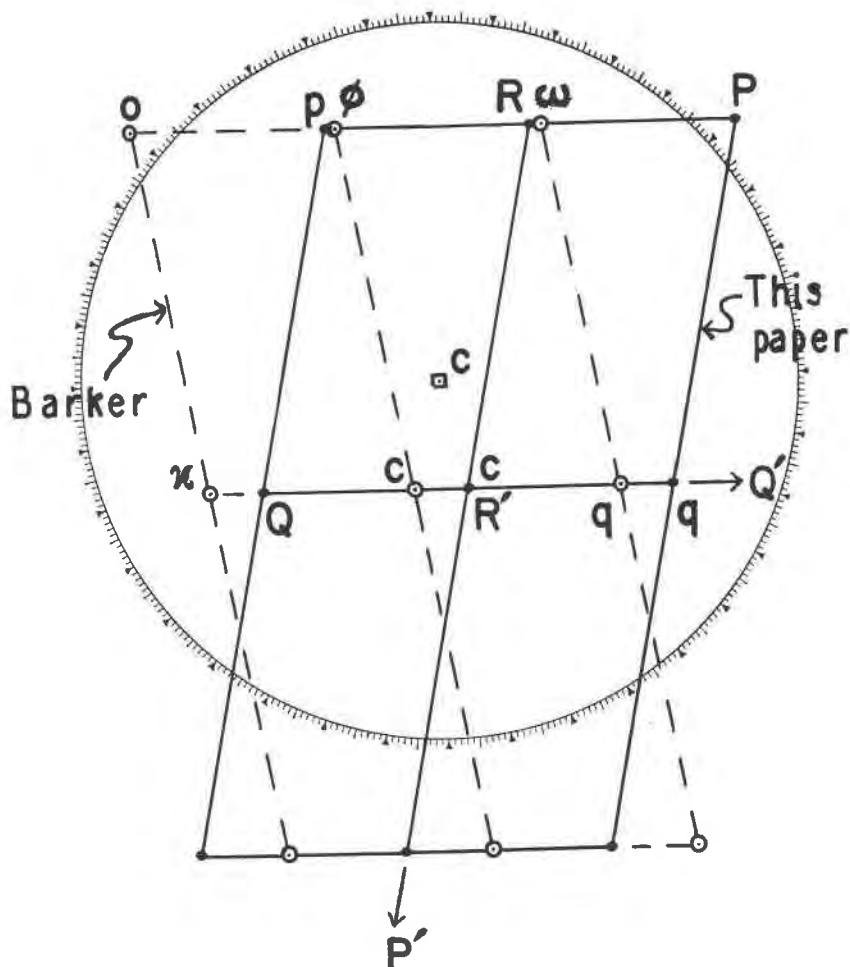


FIG. 5. Gnomonogram normal to the  $[c]$ -axis to fit the Barker setting (face-poles are open circlets, zone-lines are dashed) and the setting of this paper (face-poles are solid circlets, zone-lines are continuous).

take a model of the crystal held in the Barker position and rotate it  $180^\circ$  on  $[b^*]$  and it then has the position fitting the setting of this paper. In the Barker orientation the basal pinacoid  $c$  (001) slopes to the front

thus  $[a]$  is  $\perp [100]$ , etc. Note that just as the symbol (100) designates a crystal face parallel to the  $b$ - and  $c$ -axes, so the symbol  $[100]$  designates a plane of the reciprocal lattice parallel the  $b^*$ - and  $c^*$ -axes at a distance  $d^*_{[100]}$  (measured along the  $a$ -axis) from the origin.

and to the left; in the setting of this paper it slopes to the front and to the right. Since synthetic crystals generally lack this form (Mäder, 1942, p. 198), and in any case it is small, the crystal was first oriented by Häüy (see Goldschmidt, 1918) with the large end face sloping to the front and right. Kupffer (1826), whose measurements were standard until Barker's work, used Häüy's orientation.

Sometime not long after the middle of the 19th century the setting of this paper was adopted, and it was the standard setting b.B. (before Barker). Groth (1874, p. 35) had it in 1874; probably Rammelsberg (see Tutton, 1922, p. 282) or Kobell (see Goldschmidt, 1918) used it as early as 1855 or 1856. It seems to have been used last in an article dealing mainly with twinning (Boeris, 1905). Why did Groth decide that a change should be made (see Groth, 1895, p. 340 and 1905, p. 349)?

Groth (1908) lists 10 isomorphous triclinic pentahydrates of bivalent metal sulfates, etc., the  $A''ZO_4 \cdot 5H_2O$  compounds. These are mainly sulfates and selenates of Mn and Cu, but also of Mg, Co, Fe, and Zn (including the chromate and molybdate of Mg). He has them all in the same orientation, that of Barker for chalcantinite. It is likely that some of these were already described in the Barker orientation.

There is also another possibility, which is as follows. When one grows a synthetic chalcantinite crystal, better faces may develop on one end than on the other. The morphologist would of course mount the end with the poorer faces against the pin of his goniometer head. He would think of the  $+ [c]$ -axis as extending out from his goniometer head. Then having measured and projected the crystal, he would find that his stereogram or gnomonogram fitted the setting adopted by Barker; to convert it to the setting of this paper he would need to reflect everything in (010), which is equivalent to rotating a centro-symmetric crystal  $180^\circ$  on  $[b^*]$ . If these crystals grow with a certain end having the better terminal faces, this may imply that the crystal is not centro-symmetric. In any case, the crystal used by the writer fitted this concept. Evidently this was also Tutton's (1922, pp. 282-283) experience, since he regarded Groth's pre-1905 values for  $\alpha$  and  $\gamma$  as "the supplements of the true values," apparently not realizing that these earlier Groth values were the ones that fitted the orientation then used by Groth (1895, Fig. 184), and which is here adopted. Years later Winchell (1931, p. 233) seems to have made a similar error, which persists in his most recent book (Winchell, 1951, p. 160).

In summary, it thus seems that chalcantinite can be taken from the Barker orientation and returned to its earlier setting, which is in accordance with Donnay's rules, with a minimum of confusion. The transformation between the two settings is a very simple one. The axial ratios

are the same for the two, as is  $\beta$ . In the Barker setting  $\alpha$  is acute,  $\gamma$  is obtuse; in the setting of this paper,  $\alpha$  and  $\gamma$  are the supplements of their values in the Barker orientation. The optical goniometer measurements in the literature yield elements (orientation of this paper) as shown in Table 3.

TABLE 3. CHALCANTHITE ELEMENTS (OPTICAL GONIOMETRY)

	<i>a</i>	<i>b</i>	<i>c</i>	$\alpha$	$\beta$	$\gamma$
Kupffer	.5656	: 1 :	.5507	97°39'	106°49'	77°37'
Barker	.5721	: 1 :	.5554	97°55'	107°08'	77°19'
Tutton	.5715	: 1 :	.5575	97°44'	107°26'	77°20'
Mäder	.5689	: 1 :	.5549	97°37'	107°16'	77°25'
Average	.5695	: 1 :	.5546	97°44'	107°10'	77°25'
±	.0039		.0039	0°11'	0°21'	0°12'

## X-RAY DATA. PRECESSION ALONG TWO AXES

Many x-ray photographs of the synthetic chalcantinite crystal were taken using a number of different techniques and radiations. The crystal was oriented with  $[c]$  along the axis of a goniometer head in the ordinary manner on a two-circle optical goniometer, and a preliminary gnomonogram was prepared and its face-poles were indexed; compare Fig. 5.

For x-ray precession work, it is essential that a reciprocal axis be parallel to the axis of the goniometer head; this orientation for  $[c^*]$  was attained by the stereographic technique (Fisher, 1951). The goniometer head was then attached to the dial (vertical circle) axis of the precession camera (Fig. 6) and this axis was adjusted in azimuth (dial reading) so that, with the  $\mu$ -arc set at 0°, the direct x-ray beam went along  $[a]$  or along  $[b]$ . Approximate dial readings to attain these ends were calculated from data taken from a preliminary stereogram rotated so that  $[c^*]$  lay at the center of the primitive; refined values were given by the precession orientation technique discussed ahead.

Zero-level films for these two precessing axes taken at  $\mu = 20^\circ$  and  $30^\circ$  with Mo  $K_\alpha$ , Cu  $K_\alpha$ , and Fe  $K_\alpha$  radiations were measured, giving the results presented in Table 4.<sup>7</sup> The general appearance of such films is shown in Figs. 7*a* and 8*a*, if the 1-level spots are omitted from these. The films were given different values (as shown in Table 4) in terms of computing the weighted averages in accord with the sharpness of the spots or the size of the  $\mu$ -angle. The Mo  $K_\alpha$  films marked "double ex-

<sup>7</sup> The precession camera was set for  $F = 6.00$  cms., but calibration showed this to be actually 5.985 cms. All film measurements in Tables 4 and 6 thus represent averaged read values multiplied by the factor 1.0025, so that  $F$  may be taken as just 6.00.

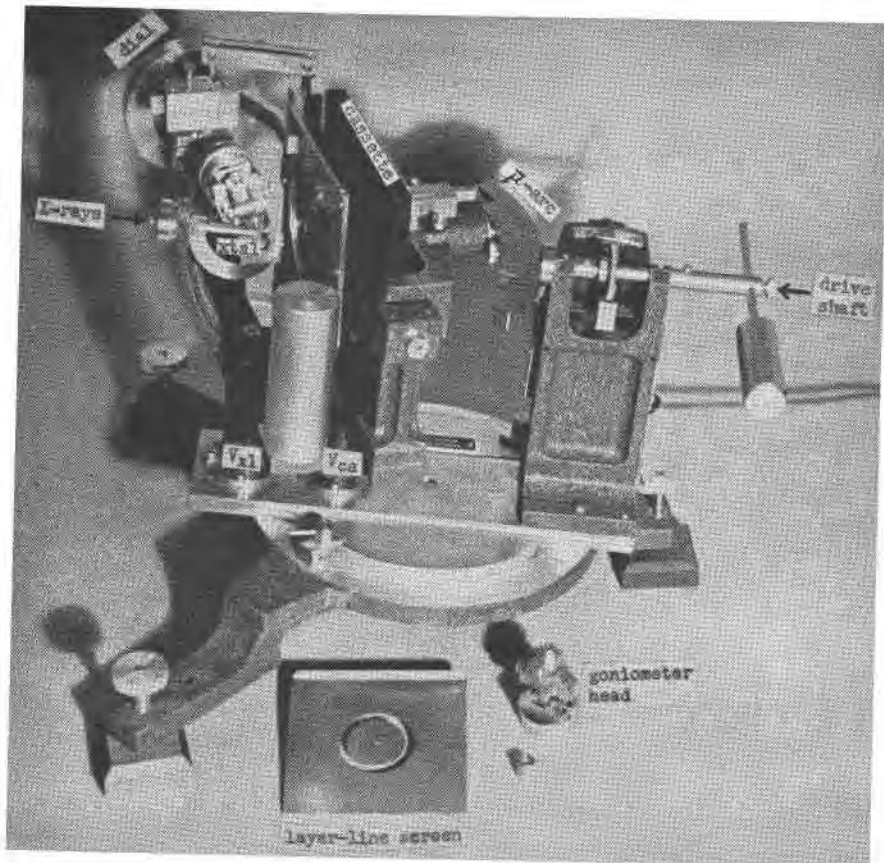


FIG. 6. The Buerger precession camera with the  $\mu$ -arc set to  $20^\circ$ .

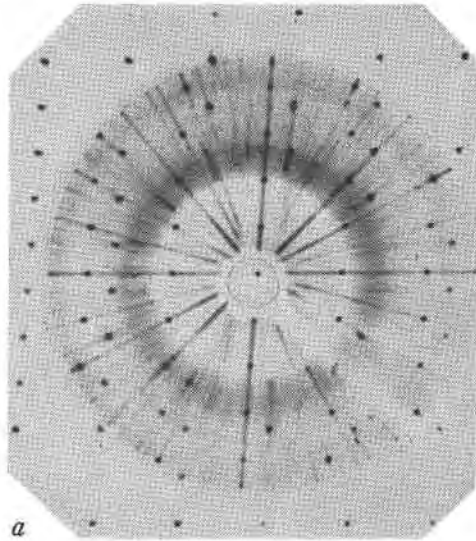
posure" were taken with a number of quartz spots which permitted calibration. All told, the results from 15 films are here presented.

These were studied on the measuring device shown by Buerger (1945, p. 553). This results in enlarged reciprocal lattice translation<sup>8</sup> values (in cms.) normal to reciprocal lattice axes in the plane of the film. For a triclinic crystal of course these are not enlarged reciprocal lattice spacings ( $d^*$ ). Each film was measured in four azimuth positions, and the checked averaged results are given in Table 4. The pictures were taken over a period of about a year; differences shown are due in part to varying conditions of humidity and temperature, but buckling of the film (which is loose at the center) is serious at times, according to F. Laves, even with

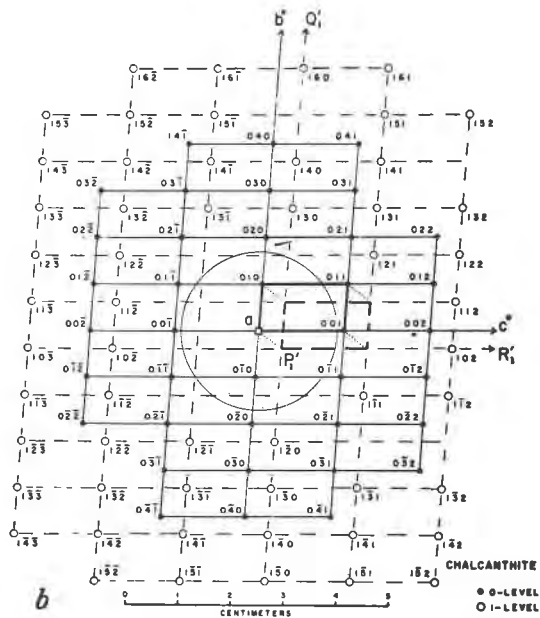
<sup>8</sup> In the triclinic these are really "spacing" values between reciprocal lattice *lines* (the lines are parallel the reciprocal axes in the plane of the film).

TABLE 4. CHALCANTHITE MEASUREMENTS (F=6.000 CMS.)

Radiation	Average Weight	Precession on [a]			Precession on [b]		
		$\alpha^*$	$t^*_{\perp b}$	$t^*_{\perp c}$	$t^*_{\perp a}$	$t^*_{\perp a}$	$\beta^*$
Mo	10	85°51'	.7506	.4059	.7109	.7214	73°49'
Mo	8				.7164	.7205	73°53'
Mo	6				.7194	.7275	73°53'
Mo	6				.7154	.7164	74°03'
Mo	4	85°53'	.7526	.4084			
Mo	Wt. Av.		.7512	.4066	.7150	.7214	
Mo	Double Ex.	85°53'	.7506	.4088	.7183	.7225	73°52'
Mo	Wt. Av.		.7509	.4077	.7161	.7218	
Mo	a*/ $\lambda$				.17480		
Mo	b*/ $\lambda$			.09586			
Mo	c*/ $\lambda$		.17655			.17619	
Cu	10	85°53'	1.6253	0.8822	1.5504	1.5700	73°54'
Cu	10	85°55'	1.6297	0.8857	1.5499	1.5674	73°51'
Cu	2				1.5542	1.5723	73°50'
Cu	Wt. Av.		1.6275	0.8840	1.5505	1.5690	
Cu	a*/ $\lambda$				.17446		
Cu	b*/ $\lambda$			.09581			
Cu	c*/ $\lambda$		.17639			.17655	
Fe	2	85°47'	2.0548	1.1128			
Fe	1				1.9453	1.9744	73°43'
Fe	a*/ $\lambda$				.17420		
Fe	b*/ $\lambda$			.09598			
Fe	c*/ $\lambda$		.17723			.17680	
Weighted Averages	a*/ $\lambda$				.17468		
	b*/ $\lambda$			.09584			
	c*/ $\lambda$		.17650			←	
	Angles	85°53'					73°53'



a



b

FIG. 7. (a) Chalcantinite diffraction pattern with precession on  $[a]$  for the 0- and 1-levels.  $F=6.00$  cms.,  $\mu=20^\circ$ ,  $\text{Cu K}\alpha$  rad. at 45 KV. and 15 ma. (b) Reciprocal lattice 0- and 1-levels projected on the  $b^*c^*$  or the  $[100]$  plane to the same scale as (a). The 1-level corresponds to the gnomogram of the Goldschmidt method; its unit circle is also shown.



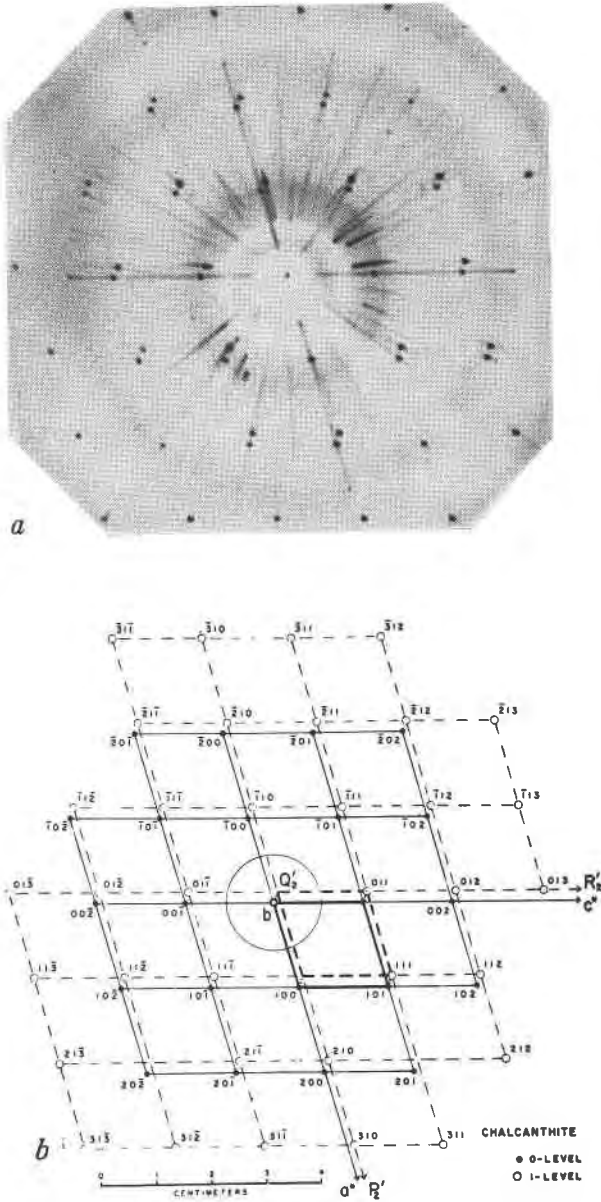


FIG. 8. (a) Chalcanthite diffraction pattern with precession on  $[b]$  for the 0- and 1-levels.  $F=6.00$  cms.,  $\mu=20^\circ$ ,  $\text{Cu K}\alpha$  rad. at 45 KV. and 15 ma. (b) Reciprocal lattice 0- and 1-levels projected on the  $a^*c^*$  or the  $[010]$  plane to the same scale as (a). The 1-level corresponds to the gnomonogram of the Goldschmidt technique; its unit circle is also outlined.

constant temperature and humidity conditions. The center of the film may be held to the metal plate backing the film cassette by a tiny spot of Duco cement, or a small alnico magnet may be inset at the center of the metal plate backing the cassette and another one placed at the center of the film outside the light-tight cover forming the front of the cassette. Or if no central spot is desired, a small screw could be put through the center of the film from the front of the cassette.

The values of  $a^*$ ,  $b^*$ , and  $c^*$  for assumed unit radiation ( $\lambda = 1\text{\AA}$ .) are obtained by use of the following formulae,<sup>8a</sup> where  $F$  = the distance from the center of the film to the crystal:

*Precession on [b]*

$$a^* = t^*_{\perp c^*} / (\sin \beta^* \cdot F \cdot \lambda) \quad (30)$$

$$c^* = t^*_{\perp a^*} / (\sin \beta^* \cdot F \cdot \lambda) \quad (31)$$

*Precession on [a]*

$$b^* = t^*_{\perp c^*} / (\sin \alpha^* \cdot F \cdot \lambda) \quad (32)$$

$$c^* = t^*_{\perp b^*} / (\sin \alpha^* \cdot F \cdot \lambda) \quad (33)$$

Given the results for these three reciprocal lattice translations, as well as the values of  $\alpha^*$  and  $\beta^*$ , all shown at the bottom of Table 4, it was still necessary to secure one more parameter before the desired triclinic calculations could be carried out. Moreover it was hoped that re-mounting of the crystal could be avoided.

Of course since  $\gamma = [a] \wedge [b]$ , it is possible to obtain this angle by taking the difference in dial readings for precession on  $[a]$  and on  $[b]$ . Since the dial circle is only 9 cms. in diameter, graduated to degrees with a 5-minute vernier, it seemed doubtful that this would lead to an accurate result. However two series of precession orientation pictures (Buerger, 1944, pp. 21-26) were made two weeks apart as shown in Fig. 9. The dial readings were taken (estimating to the nearest minute) before each picture was started and again, independently, after each picture was completed. For the eight pictures three identical results were obtained, three differed by  $1'$ , one differed by  $2'$  and inadvertently but one reading

<sup>8a</sup> Other formulae of interest in this connection are as follows:

*Precession on [c]*

$$a^* = t^*_{\perp b^*} / (\sin \gamma^* \cdot F \cdot \lambda) \quad (34); \text{ and } a = (F\lambda) / (t^*_{\perp b^*} \sin \beta) \quad (34')$$

$$b^* = t^*_{\perp a^*} / (\sin \gamma^* \cdot F \cdot \lambda) \quad (35); \text{ and } b = (F\lambda) / (t^*_{\perp a^*} \sin \alpha) \quad (35')$$

<p><i>Precession on [b]</i></p> $a = (F\lambda) / (t^*_{\perp c^*} \sin \gamma) \quad (30')$ $c = (F\lambda) / (t^*_{\perp a^*} \sin \gamma) \quad (31')$	<p><i>Precession on [a]</i></p> $b = (F\lambda) / (t^*_{\perp c^*} \sin \gamma) \quad (32')$ $c = (F\lambda) / (t^*_{\perp b^*} \sin \beta) \quad (33')$
---	--

was made on one (that at the upper right). Averaged values are given.<sup>9</sup>

In the precession orientation technique, in which no screen is placed in the layer-line screen holder, the ends of the zero-level general radiation streaks outline the circumference of a circle of precession, of which the streaks themselves should be the radii or spokes, providing precession is occurring exactly along a translation direction of the direct lattice. This is rarely the case, however, since it is very difficult to make a precession camera in which the dial axis is exactly normal to the direct  $x$ -ray beam (when  $\mu=0^\circ$ ).<sup>10</sup> On the instrument used in this study, when the crystal is in perfect orientation the center of this diffraction circle is 0.8 mm. (corresponds to 23 minutes) to the right of the center of the hub (the point where the "spokes" meet) under the conditions stated in the caption of Fig. 9. Scratches made along the streaks on the film intersect at the hub-center, (the direct-beam spot), and a needle-prick appears at the center of the circle of precession. This latter point is determined easily by placing the film on a light box topped with a glass positive made from polar coordinate paper. It will be noted that streaks in the two left pictures of Fig. 9 correspond to those of the zero-level of Fig. 7*a* and those in the right-central pictures of Fig. 9 correspond to the 0-level streaks of Fig. 8*a*.

As the "east-west" streaks of Fig. 9 trace out  $[c^*]$ ,<sup>11</sup> it is only necessary to note the relation of the needle-prick at the center of the diffraction circle to the trace of  $[c^*]$  to find the error in the dial setting. Since with an error of  $1^\circ$  there is a streak difference of 4.2 mm. (difference in length of a "north spoke" and a "south spoke") where  $F=6.00$  cms. and the orientation error is small, this is easily calculated. Thus in the left-center picture (upper row of Fig. 9) since the needle-prick is 0.50 mm. below the trace of  $[c^*]$ , the dial reading must be increased from the value given by  $(2 \cdot 0.5 \cdot 60)/4.2 = 2 \cdot 0.5 \cdot 14.3 = 14'$  to have precession exactly along  $[\bar{a}]$ . In this way averaged dial readings for precession along  $[\bar{b}]$  and  $[a]$  were obtained. The corrected values for the two left-hand pairs of pictures (subtracting  $180^\circ$  from the  $[\bar{a}]$  values) were  $48^\circ 52'$ ,  $48^\circ 58'$ ,  $48^\circ 54'$ , and  $48^\circ 56'$ . For the two right-hand pairs the results were  $126^\circ 20'$ ,  $126^\circ 22'$ ,

<sup>9</sup> In actual practice it is better to take double exposures made when dial readings are approximately  $180^\circ$  apart. One exposure has twice the time of the other, so that the two are easily differentiated. If there is any difficulty in interpreting this, a new picture is made with the (approximately) horizontal arc of the goniometer head about one degree off its position for true orientation. Such pictures are not very good for illustration purposes. thus the principle is here elucidated by single exposure as shown in Fig. 9.

<sup>10</sup> The latest model precession instrument (Fig. 6) has a collimator which is adjustable for both height and direction.

<sup>11</sup> All  $x$ -ray photos are shown just as they appear looking at the film in the cassette from the  $x$ -ray source with the dial on the left.

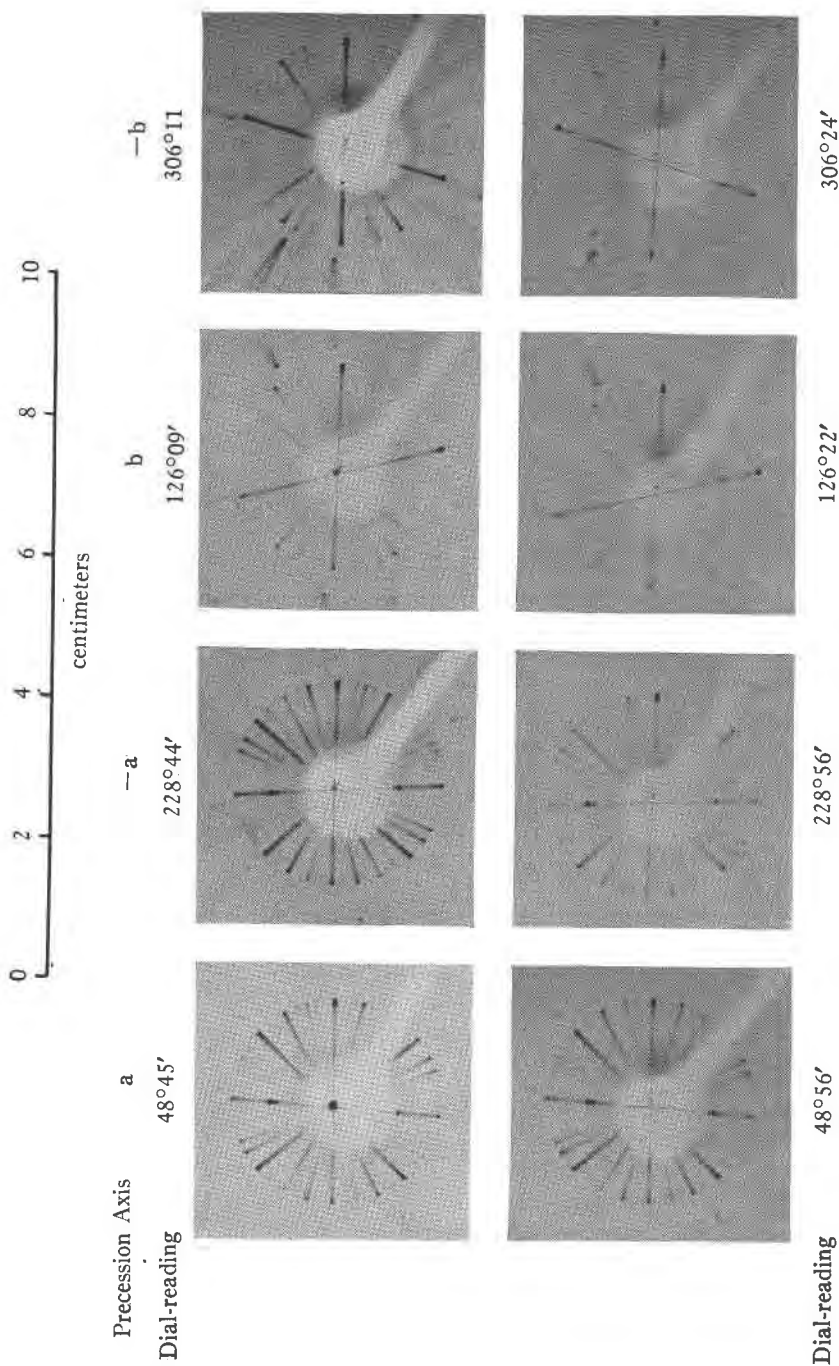


FIG. 9. Precession orientation pictures of chalcantinite with  $[c^*]$  the dial axis. The dial reading is indicated for each example. The differences for the averaged dial readings for precession along  $[a]$  and  $[b]$  indicate that  $\gamma = 7726'$ .  $F = 6.00$  cms.,  $\mu = 7^\circ$ , unfiltered Cu rad. at 45 KV. and 15 ma.

126°19', and 126°21'. This yields an average value for  $\gamma$  of 126°20½' - 48°55' = 77°25½'. It seems likely that the probable error in the  $\gamma$  value does not exceed 3', which may give this reading about the same order of accuracy as those for  $\alpha^*$  and  $\beta^*$  as shown at the base of Table 4.

Given  $a^* = 0.1747$ ,  $b^* = 0.0958$ ,  $c^* = 0.1765$ ,  $\alpha^* = 85^\circ 53'$ ,  $\beta^* = 73^\circ 53'$ , and  $\gamma = 77^\circ 26'$ , the elements for chalcantinite can be calculated using standard formulae (for example see Buerger, 1942, pp. 360-361). The results are given in Table 5, along with those of previous workers employing *x*-ray techniques. Angles used by earlier *x*-ray workers are those of Table 3. Barth and Tunell (1933) found  $\alpha^* = 85^\circ 48'$ ,  $\beta^* = 74^\circ 00'$ , and  $\gamma^* = 100^\circ 45'$ ; however they considered Tutton's angles to be better than these. The writer's figures yield  $\alpha = 97^\circ 34'$ ,  $\beta = 107^\circ 17'$ ,  $\gamma^* = 100^\circ 52'$ .

TABLE 5. CHALCANTHITE ELEMENTS (X-RAY GONIOMETRY)<sup>12</sup>

Name	Date	$a_0$	$b_0$	$c_0$	$a$	$b$	$c$	Technique	Angles used
G. & B.	1929	6.08	10.80	5.90	0.563	1	0.546	Rotation	Barker
B. & T.	1933	6.122	10.695	5.96	.5725	1	.5575	Weiss.	Tutton
B. & L.	1934	6.13	10.7	5.98	0.572	1	0.558	Rotation	Tutton
D. J. F.	1952	6.104	10.72	5.949	.5693	1	.5548	Precession	D. J. F.

A graph of the results obtained by various workers appears in Fig. 10; in this the data of Gossner and Brückl (1929) and of Beevers and Lipson (1934) are not shown, because neither of these pairs was interested in accuracy better than about one per cent. The very close agreement between the writer's values and those of Mäder (1942) is here emphasized.

#### X-RAY DATA. PRECESSION ALONG ONE AXIS

What is probably the most accurate general technique for determining the elements of a triclinic crystal from a single setting on the precession camera has just been described; this involved precession along two directions. It is perhaps worth emphasizing that precession along one crystal axis furnishes sufficient data to obtain these elements, providing one gets an *n*-level pattern. This is brought out from Figs. 7 and 8; these should be compared with Figs. 2*b* and 3*b* of the previous paper (Fisher, 1952). The method of obtaining the triclinic elements from a picture made by precession on a single axis may be illustrated by the example of Fig. 7. The close similarity between Fig. 7*b* and Fig. 2*b* becomes clearer if the

<sup>12</sup> Corrected to fit wave lengths where (kX units)  $\cdot 1.00202 = \text{\AA}$  units. Cf. *Am. Mineral.*, 32, 591-592 (1947).

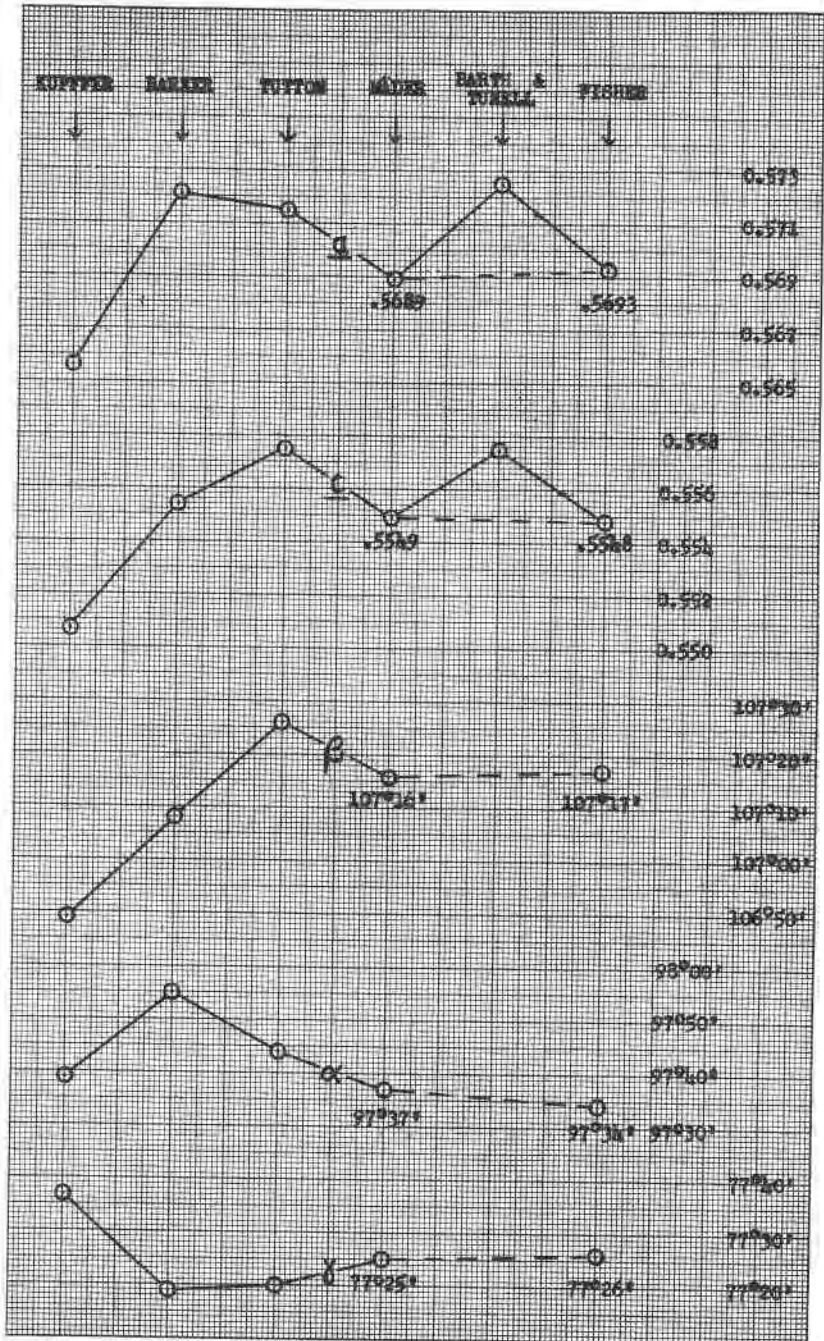


FIG. 10. Graph showing values obtained for chalcantite elements.

former is rotated  $180^\circ$  about  $[c^*]$ .<sup>13</sup> Before a 1-level picture such as is shown in Fig. 7*a* can be made, it is necessary to know the reciprocal spacing  $d^*_{1100} = \lambda/a_0$ . This can be obtained from a cone-axis photograph (Buerger, 1944, p. 8).<sup>14</sup> Having such an  $n$ -level precession pattern, one can measure values that are analogous to the projection constants of the Goldschmidt two-circle technique. For the films of Figs. 7*a* and 8*a* these were as shown in Table 6.

TABLE 6. FILM MEASUREMENTS (in cms.)

Fig. 7 <i>a</i>	Fig. 8 <i>a</i>	Special film <sup>a</sup>
$d^*_{1100} = \lambda/a = 0.2526$	$d^*_{1010} = \lambda/b = 0.1438$	$2d^*_{1010} = 0.2876$
$\alpha^* = 85^\circ 51'$	$\beta^* = 73^\circ 53'$	$\beta^* = 75^\circ 54'$
$t^*_{\perp c^*} = 0.887$	$t^*_{\perp c^*} = 1.546$	$t^*_{\perp c^*} = 1.549$
$t^*_{\perp b^*} = 1.627$	$t^*_{\perp a^*} = 1.555$	$t^*_{\perp a^*} = 1.562$
$aG_1' = 0.332$ (cf. $Y_1'$ )	$bE_2' = 0.109$ (cf. $Z_2'$ )	$bE_2' = 0.112$ (cf. $Z_2'$ )
$aF_1' = 0.464$ (cf. $S_1'$ )	$bG_2' = 0.188$ (cf. $S_2'$ )	$bG_2' = 0.190$ (cf. $S_2'$ )

<sup>a</sup> The results in this column were measured from a film identical with that of Fig. 8*a* except that the 2-level was taken in place of the 1-level; thus the values shown for the bottom two figures in this column are half those actually measured.

The bottom two values in Table 6 for Fig. 7*a* represent the components of the shear between the 0- and 1-levels of the reciprocal lattice in directions normal to the  $[c^*]$ - and  $[b^*]$ -axes respectively. Thus these are the central distances of the common points; see Fig. 2*d* of the previous paper. Using formulas (32) and (33) with the values given in Table 6 for Fig. 7*a* yields  $b^*$  and  $c^*$ . Similarly formulas (14) and (15) of the previous paper furnish  $\beta$  and  $\gamma$ , if one remembers that  $r = F \cdot d^*_{1100} = 1.515$  cms. From the six parameters now available (shown in italics in the two lines marked Row 1 of Table 7), the other values given in Row 1 of Table 7 were calculated by standard procedures. The results shown in the second and third rows of Table 7 were derived in analogous fashion from the data given in the middle and right-hand columns of Table 6.

The last row in Table 7 contains the assumed best values for chalcantite, obtained as described in an earlier section of this paper by using precession photos taken along both the  $[a]$  and  $[b]$  axes. The weakness of the single axis precession picture technique would seem to be that the shear-components between adjacent layers of the reciprocal lattice must be used for findings  $\gamma$  and  $\alpha$  or  $\beta$ . While these components are given to

<sup>13</sup> To make Fig. 8*b* fit Fig. 3*b* rotate the former  $74^\circ$  anticlockwise on  $[b]$  and then  $180^\circ$  about  $[a^*]$ .

<sup>14</sup> While the reciprocal spacing value obtained from a cone-axis photograph does not have great precision, the first result can be refined by the precession technique; see Buerger (1944, pp. 27-32).

TABLE 7. RESULTS OF COMPUTATIONS

Row	Film	$\alpha$	$\beta$	$\gamma$	$\alpha^*$	$\beta^*$	$\gamma^*$
1	Fig. 7a	97°29'	107°02'	77°38'	85°51'	74°07'	100°43'
2	Fig. 8a	97°12'	107°13'	77°42'	86°12'	73°53'	100°42'
3	Special	97°24'	107°14'	77°35'	86°00'	73°54'	100°46'
4	Best Values	97°34'	107°17'	77°26'	85°53'	73°53'	100°52'
Row	Film	$a$	$b$	$c$	$a^*$	$b^*$	$c^*$
1	Fig. 7a	6.105	10.68	5.95	0.1744	0.0961	0.1763
2	Fig. 8a	6.12	10.72	6.00	0.1740	0.0956	0.1750
3	Special	6.12	10.72	5.97	0.1743	0.0958	0.1758
4	Best Values	6.104 <sub>5</sub>	10.72	5.949	0.1747	0.0958	0.1765

0.01 mm. in Table 6, the order of their accuracy is probably only about 0.03 mm., though this might well be improved if several films were measured, and if each of these was taken by a technique that inhibited any buckling. Any errors due to temperature or humidity changes could be cancelled out by taking a pattern of a standard sample (halite or quartz) on each film.

#### COMPARISON WITH TWO-CIRCLE GONIOMETRY

Those familiar with the Goldschmidt technique will recognize the close similarity between the gnomonogram given by this and the 1-level precession film, as well as the calculations based on these. Of course the  $x$ -ray method yields the absolute size of the unit cell, and thus the results given by it far exceed in value those obtainable from the optical goniometer. The latter is a superseded instrument as far as determination of the fundamental geometrical crystal constants is concerned. But the Goldschmidt method is still a fine training tool for those who wish to study  $x$ -ray methods first by the precession camera, later by the Weissenberg. It will continue to be fundamental in morphologic and habit studies. The optical goniometer is often useful in preliminary orientation work. For these reasons the writer has computed an angle table (Table 8) based on the measurements herein reported. The stereogram of Fig. 11 gives the position of the optical indicatrix<sup>15</sup> in the present setting using

<sup>15</sup> The optic triangle is an equilateral right-angled spherical triangle representing an indicatrix octant. The arcs bounding it can be drawn readily by plotting its apices both cyclographically and eothygraphically in a single projection (from the position angles given in Table 8). The apices of the *gnom*-optic triangle are the centers of the required arcs.



the results of Mäder (1942). Figure 12 shows a model representing the unit cell (lucite sheets; scale 1 inch = 1 Å.) and 8 cells of the reciprocal lattice (nodes on wire rods; same scale) to fit Mg K $_{\alpha}$  radiation of  $\lambda = 9.889\text{Å.}$ ;

TABLE 8. CHALCANTHITE: CuSO $_4 \cdot 5\text{H}_2\text{O}$ Triclinic, P $\bar{1}$ 

$$a:b:c=0.569:1:0.555; \alpha=97^{\circ}34', \beta=107^{\circ}17', \gamma=77^{\circ}26'$$

$$p_0:q_0:r_0=0.994:0.543:1; \alpha^*=85^{\circ}53', \beta^*=73^{\circ}53', \gamma^*=100^{\circ}52'$$

$$p_0'=1.0441, q_0'=0.5700, x_0'=0.3111, y_0'=0.0754, m_0=0.1869, n_0=0.9735$$

No. <sup>a</sup>	Form	$\phi$	$\rho$	A	B	C	Barker
1	$c(001)$	76°22'	17°45½'	73°53'	85°53'	00°00'	$c(001)$
2c	$b(010)$	00 00	90 00	100°52	00°00'	85 53	$b(010)$
3b	$a(100)$	100 52	90 00	00 00	100 52	73 53	$a(100)$
4	$n(130)$	34 07	90 00	66 45	34 07	76 57	$\pi(1\bar{3}0)$
5d	$h(120)$	47 24	90 00	53 28	47 24	74 31	$\lambda(1\bar{2}0)$
6c	$m(110)$	70 00	90 00	30 52	70 00	72 21	$\mu(1\bar{1}0)$
7	$d(210)$	85 05	90 00	15 47	85 05	72 27	$\nu(2\bar{1}0)$
8	$F(3\bar{1}0)$	110 40	90 00	9 48	110 40	75 25	—(310)
9	$T(2\bar{1}0)$	115 10	90 00	14 18	115 10	76 15	—(210)
10a	$M(\bar{1}10)$	126 48	90 00	25 56	126 48	78 48	$m(110)$
11	$L(1\bar{2}0)$	142 31	90 00	41 39	142 31	82 56	$l(1\bar{2}0)$
12	$N(1\bar{4}0)$	157 31	90 00	56 39	157 31	87 20	$p(1\bar{4}0)$
13d	$w(021)$	14 22	51 26	87 17	40 46	45 07	$\tau(0\bar{2}1)$
14	$q(011)$	25 44	35 37	81 24	58 22	27 31	$\kappa(0\bar{1}1)$
15c	$Q(0\bar{1}1)$	147 50	30 18	69 52	115 17	29 24	$q(011)$
16b	$\bar{W}(0\bar{2}1)$	163 43	47 59	70 11	135 31	49 37	$t(021)$
17	$e(201)$	97 40	67 14	22 59	97 04	50 55	$d(201)$
18	$R(\bar{1}01)$	-69 08	37 24	126 52	77 30	52 51	$\phi(\bar{1}01)$
19	$u(141)$	31 46	68 30	70 37	37 44	56 33	—(141)
20	$x(131)$	40 04	64 17	63 56	46 25	50 36	$\psi(1\bar{3}1)$
21d	$Z(\bar{1}21)$	-26 50	57 42	121 07	41 02	63 15	$\sigma(\bar{1}21)$
22	$P(\bar{1}11)$	-40 18	47 50	125 16	55 35	57 28	$o(\bar{1}11)$
23a	$p(\bar{1}\bar{1}1)$	-112 38	37 44	120 41	103 37	55 20	$\omega(\bar{1}\bar{1}1)$
24d	$z(\bar{1}21)$	-140 33	48 20	110 56	125 14	63 12	$\xi(\bar{1}21)$
25	$X(\bar{1}\bar{3}1)$	-153 35	58 05	103 09	139 29	72 55	$\zeta(\bar{1}\bar{3}1)$
	Direction						
	$\alpha(\text{Na})$	168 47	75 53	68 37	162 02	77 18	
	$\beta$	75 25	76 51	28 27	75 48	59 06	
	$\gamma$	-55 03	19 29	107 44	78 59	33 51	
	A $_1$	-17 42	76 44	117 44	22 00	78 37	
	A $_2$	177 17	48 46	79 50	138 42	54 15	
	[ $c$ ]	—	00 00	90 00	90 00	17 45½	
	[ $b$ ]	-169 08	82 26	90 00	166 47	90 00	
	[ $a$ ]	-90 00	72 43	159 40	90 00	90 00	

<sup>a</sup> The letters in this column give a crude idea of the relative importance of the various forms. Those marked (a) are most important, the (b) ones are of lesser importance, etc.

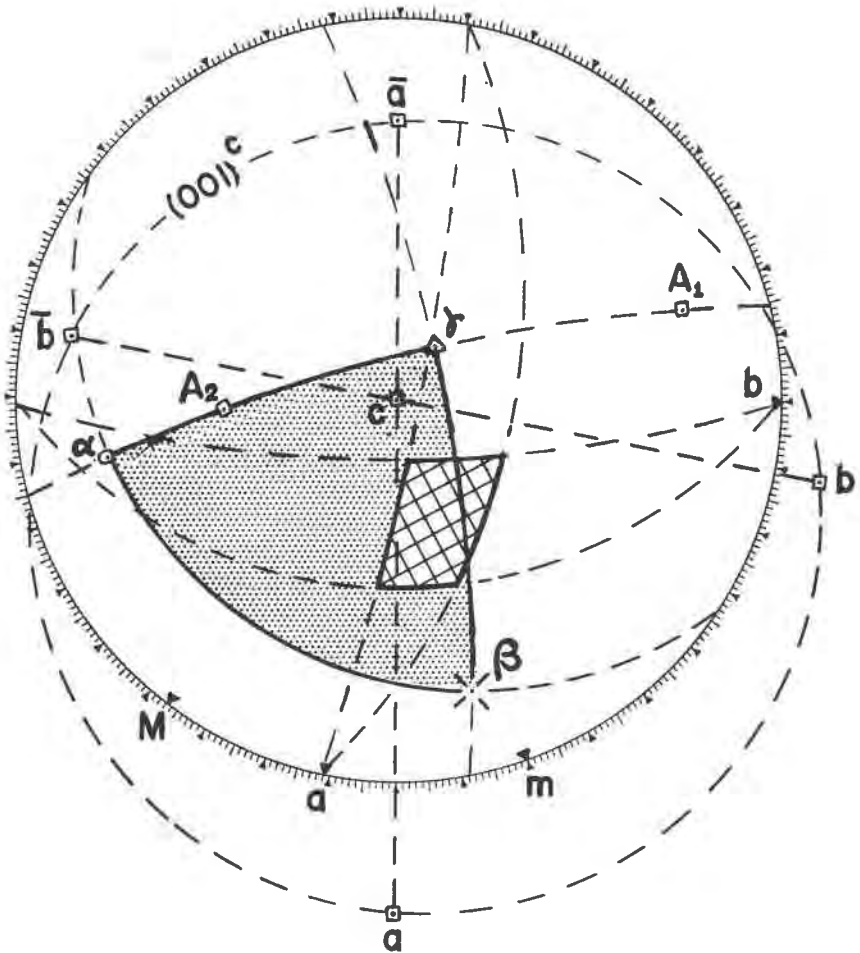


FIG. 11. Stereogram of chalcantite showing indicatrix directions, standard orientation. The optic triangle is stippled and the primitive stereogram is reticulated.

thus  $a^* = 1.7255$ ,  $b^* = 0.9472$ , and  $c^* = 1.7446$  Å. In the picture the  $c$ -axis is vertical and the view is from the upper right octant. The model may be fitted into its support base with any axis vertical. In each case some plane of the reciprocal lattice is horizontal. Similarly it is clear that the wires of the reciprocal lattice network are normal to the pinacoid faces. Or the model may be held in the two hands by the opposite ends of any axis and slowly rotated or oscillated. If one imagines a sphere of reflection to be present, it is then easy to visualize the development of the straight layer lines.

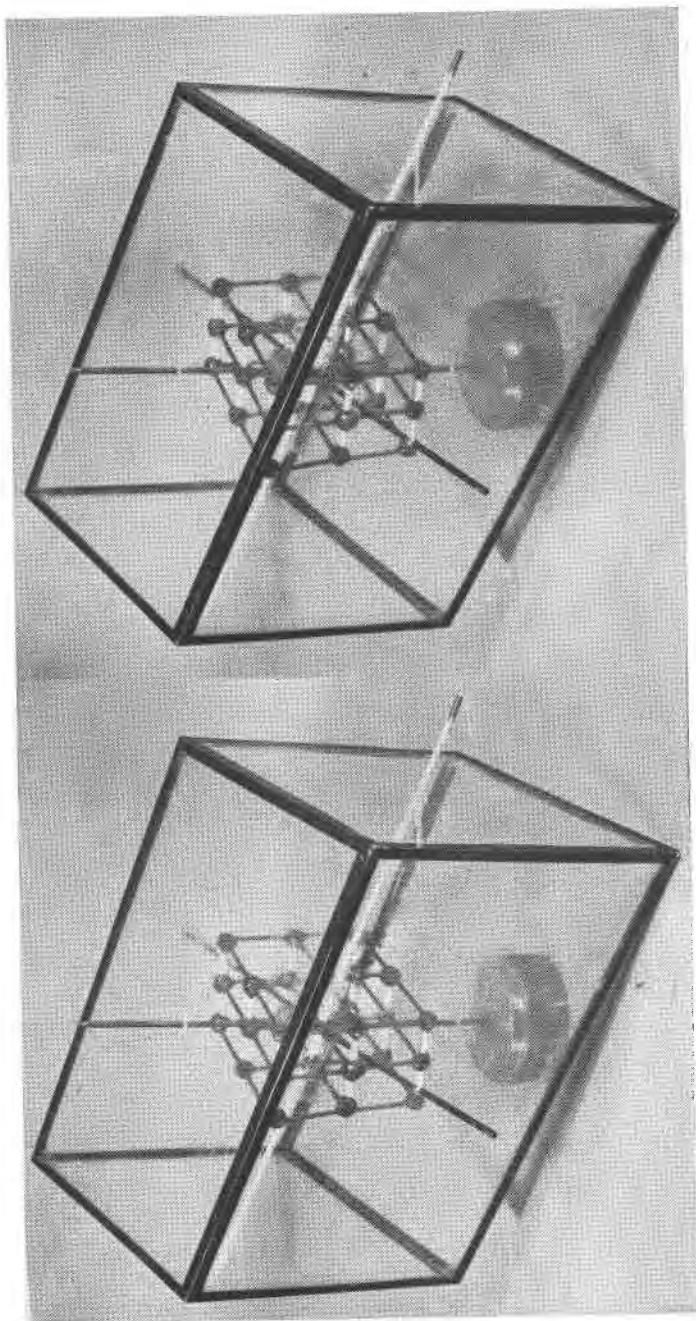


FIG. 12. Stereo-photograph of a model of the chalcantite unit cell containing a portion of the chalcantite reciprocal lattice.

*Acknowledgments:* F. L. Koucky and B. P. Asanachinta helped with the drawings, and W. F. Schmidt did the photography. The members of two classes (and particularly F. D. Bloss) served as stimulating subjects.

## REFERENCES

- BARKEE, T. V. (1922), Graphical and Tabular Methods in Crystallography, London.  
 ——— (1930), The Study of Crystals, London.
- BARTH, T. F. W., AND TUNELL, G. (1933), The space-lattice and optical orientation of chalcantite: *Am. Mineral.*, **18**, 187-194.
- BEEVERS, C. A., AND LIPSON, H. (1934), Crystal structure of copper sulphate pentahydrate: *Proc. Royal Soc. (London)*, **146A**, 570-582.
- BOERIS, G. (1905), Osservazioni cristallografiche sopra il Solfato di Rami: *Atti d. Soc. ital. sc. nat. Milano*, **44**, 73-85. Reprinted in 1907: *Riv. min. crist. ital. (Padova)*, **33**, 5-17. Cf. *Zeit. Krist.*, **43** (1906), 489-490.
- BUERGER, M. J. (1942), *X-ray Crystallography*, New York.  
 ——— (1944), The photography of the reciprocal lattice: *Am. Soc. X-ray and Electron Diffr., Monogr. 1*, 37 pp.  
 ——— (1945), Soap crystals: *Am. Mineral.*, **30**, 551-571.
- DANA, E. S. (1892), *A System of Mineralogy*, p. 944, New York.
- DONNAY, J. D. H. (1943*a*): Rules for the conventional orientation of crystals: *Am. Mineral.*, **28**, 313-328.  
 ——— (1943*b*), Resetting a triclinic unit-cell in the conventional orientation: *Ibid.*, 507-511.
- FISHER, D. J. (1951), Setting a given direction parallel to the axis of a goniometer head: *Am. Mineral.*, **36**, 123-128.  
 ——— (1952), Triclinic gnomonostereograms: *Ibid.*, **37**, 83-94.
- GOLDSCHMIDT, V. (1897), *Winkeltabellen*, 210, Berlin.  
 ——— (1918), *Atlas der Kristallformen*, 5, Heidelberg.  
 ——— (1934), *Kursus der Kristallometrie*, Berlin.
- GOSSNER, B. v. BRÜCKL, K. (1929), Die Gitterkonstanten von Kupfervitriol: *Zeit. Krist.*, **69**, 422-426.
- GROTH, P. (1874), *Tabellarische Uebersicht der Mineralien*, Braunschweig.  
 ——— (1895), *Physikalische Krystallographie*, Leipzig.  
 ——— (1905), *Ibid.*, Leipzig.  
 ——— (1908), *Chemische Krystallographie*, 2, Leipzig.
- KUPFFER, A. F. (1826), Ueber die Krystallisation des Kupfervitriols, etc.: *Pogg. Ann.*, **8**, 215-229.
- MÄDER, J. (1942), Kristallographie und Optik des Kupfervitriols: *Schweiz. Min. u. Petr. Mitt.*, **22**, 197-232.
- MILNE, I. H., AND NUFFIELD, E. W. (1951), Vandenbrandeite: *Am. Mineral.*, **36**, 394-410.
- PALACHE, C., BERMAN, H., AND FRONDEL, C. (1951), *The System of Mineralogy of J. D. and E. S. Dana*, Vol. 2, New York.
- TERPSTRA, P. (1946), *Kristallographie*, Groningen.
- TUTTON, A. E. H. (1911), *Crystallography and Practical Crystal Measurement*, London.  
 ——— (1922), *Ibid.*, London.
- WINCHELL, A. N. (1931), *The Microscopic Characters of Artificial Inorganic Solid Substances or Artificial Minerals*, New York.
- WINCHELL, A. N. (1951), *Elements of Optical Mineralogy, Part II*, New York.

*Manuscript received Aug. 14, 1951.*